Radiation engineered copper nanoparticles immobilised catalytic reactor (Cu-NICaR) system

Swarnima Rawat[1], Nilanjal Misra[1], Virendra Kumar[1,2]*, Shubhangi Atmaram Shelkar[1], Narender Kumar Goel[1], Rakesh Kumar Singhal[3], Lalit Varshney[1,2]

[1]Radiation Technology Development Division, Bhabha Atomic Research Centre, Trombay, Mumbai 400085, India
[2]Homi Bhabha National Institute, Anushaktinagar, Mumbai 400094, India
[3]Analytical Chemistry Division, Bhabha Atomic Research Centre, Trombay, Mumbai 400085, India

*Corresponding author

DOI: 10.5185/amlett.2018.2123
www.vbripress.com/aml

Abstract

A robust and reusable Copper Nanoparticles Immobilised Catalytic Reactor (Cu-NICaR) system was fabricated by immobilising Copper Nanoparticles (Cu NPs) onto a radiation functionalized polymer support. Gamma radiation induced simultaneous irradiation grafting process was employed for introducing poly-glycidyl methacrylate (poly(GMA)) chains onto non woven PE-PP matrix. Optimization of the grafting process was carried out by studying the effect of experimental parameters, such as absorbed dose, monomer concentration and solvent polarity on grafting yield. The poly(GMA)-*g*-PE-PP matrix was used as a functional polymer support for Cu NPs, synthesised under optimized conditions using $NaBH_4$ as reducing agent**.** Characterization of the samples was carried out by UV-Visible spectrophotometer, Fourier Transform Infrared (FTIR) Spectroscopy, X-ray fluorescence (XRF), Thermogravimetric Analysis (TGA) and Scanning Electron Microscopy (SEM). Catalytic activity of Cu NPs immobilised poly(GMA)-g-PE-PP catalytic system was studied by spectrophotometrically monitoring the catalytic reduction of *p*-nitrophenol (PNP), using $NaBH_4$ as reducing agent**.** The Cu NPs-immobilised-poly(GMA)-g-PE-PP was observed to exhibit excellent catalytic activity both in batch process (12 cycles over a period of 30 days) as well as in fixed bed column reactor mode, without significant loss of activity.

Keywords: Radiation grafting, copper nanoparticles, Cu-NICaR, catalyst, p-nitrophenol.

Introduction

In the past few decades, metallic nanoparticles have emerged as one of the most promising catalysts for numerous reactions. Their catalytic activity is governed by high surface area and electron density on the surface, which in turn is determined by particle size, shape and the number of coordination sites on the surface [1]. However, the primary obstacle encountered with metallic nanoparticle based catalysts is their reusability. Since separation of metallic nanoparticles from the reaction system is neither easy nor cost effective, their applications have been mostly confined to the laboratory scale. For large scale applications, a catalytic system must possess reusability and robustness. These indispensible attributes of a catalytic system make it both economically and commercially viable. One of the feasible solutions to this problem involves immobilisation of nanoparticles on a template/support, which not only permits the nanoparticles to be reused but also makes the catalytic system robust [2,3].

Among various metallic nanoparticles, copper nanoparticles have elicited great interest due to their easy availability, low cost and high surface to volume ratio. Cu exists in multiple accessible oxidation states i.e. Cu(0), Cu(I), Cu(II), and Cu(III); therefore, it can catalyze various reactions including organic transformations, photocatalytic, electrocatalytic and cycloaddition reactions, etc. [3-6]. Copper nanoparticles have also been employed as heterogeneous catalysts for numerous transformations which are important from an environmental point of view, e.g., selective reduction ~~in~~ of nitric oxide, decomposition of nitrogen dioxide, oxidation of carbon monoxide, reduction of organic pollutants, etc. [7, 8]. Additionally, some other important properties of copper, such as good conductivity, biocompatibility, antibacterial activities, electrical and sensing properties, make them even more desirable [9, 10]. However, high surface oxidation tendency of copper nanoparticles complicates their synthesis. The oxide phase is thermodynamically more stable compared to the metallic phase, thereby making copper nanoparticles extremely sensitive to air and limiting their applications [11]. Surface oxidation can be prevented either by carrying out the synthesis of

copper nanoparticles in inert atmosphere or by employing suitable stabilizing agent or capping agent. The stabilizing agent controls nucleation of particles by reducing surface energies and, therefore, act as a particle growth terminator by preventing agglomeration of nanoparticles during synthesis. Thus, the stabilizing agent serves a dual role of preventing surface oxidation of the nanoparticles as well as controlling their growth [12, 13]. Polymers or surfactants having the ability to form complexes with metal ion are generally used as stabilizing agent. Polymers can act as stabilizing agent in liquid as well as in solid state. When employed in liquid state, polymers act by creating a surface layer on nanoparticles like a capping agent, and thus, reduce their surface energies [14-16], whereas in solid state, they act as capping agent and also provide solid support/template for the nanoparticles [17-19].

Various methods have been reported in literature for synthesis of copper nanoparticles, including chemical reduction [20], thermal decomposition [21], radiolytic reduction [22], polyol method [23], hydrothermal reduction [24], reverse micelles method [25], sonochemical reduction [26], laser ablation method [27], micro-emulsion method [28], vacuum vapour deposition [29], *in situ* chemical synthesis, etc. [30]. Among these, chemical reduction is the most preferred one, owing to its simplicity, efficiency and cost-effectiveness. Moreover, better control over size and size distribution of nanoparticles can be achieved by simple optimization of various experimental parameters, such as type and concentration of reducing agent, pH, concentration of metal precursor ions, temperature, etc. [31]. In order to ensure the efficient and repeated use of catalytic system, immobilisation of catalysts onto functionalized polymer supports ~~have~~ has been reported [2,32].

In the present study, Cu-NICaR catalytic system has been fabricated by immobilisation of copper nanoparticles on radiation grafted poly(GMA)-*g*-PE-PP non-woven polymer support. Non-woven PE-PP is a suitable choice for polymer support owing to its ~~attractive~~ invaluable properties, such as high specific surface area, good mechanical strength, low cost, good chemical resistance, etc. Epoxy functional group containing poly(GMA) chains were introduced covalently onto the PE-PP surface via mutual irradiation grafting process. Radiation induced grafting is widely used to produce functionalized polymer supports, as it offers many advantages over conventional grafting methods, such as the absence of harmful chemical initiators, room temperature processing, uniform grafting, better process control and high grafting yield [33-35]. Cu^{2+} ions immobilised on the radiation grafted poly(GMA)-*g*-PE-PP support were subsequently reduced to Cu NPs by chemical reduction method, using $NaBH_4$ as reducing agent. The catalytic activity of Cu nanoparticles was studied by spectrophotometrically monitoring Cu NPs catalysed reduction of *p*-nitrophenol (PNP) at 400nm, in presence of $NaBH_4$**.**

Experimental

Materials and methods

Polyethylene-polypropylene (PE-PP) non-woven fabric (Kurashiki Senl Kako Co. Okayama, Japan.) was used as polymer support after thorough washing in ethanol and water. Glycidyl methacrylate (GMA) (Sigma-Aldrich, purity = 97%), $CuSO_4.5H_2O$ (Sarabhai Chemicals, purity = 99.5%), Sodium Borohydride ($NaBH_4$) (Sigma Aldrich, purity = 98.5%) were used as received. All aqueous solutions were prepared in ultrapure water with resistivity = 18 MΩ.cm generated using water purification system 'Ultraclear TWF UV' (SG Wasseraufbereitung & Regenerierstation GmbH, Germany). Radiation grafting experiments were carried out in a ^{60}Co gamma radiation source (GC5000, BRIT, India) having a dose rate of 1.5 kGy h^{-1}, determined using Fricke dosimetry. [36]

Radiation grafting process

Gamma radiation induced mutual irradiation grafting process was adopted for fabrication of Poly(GMA)-*g*-PE-PP support [32]. A reaction system comprising of PE-PP strip of known weight, immersed in glass-stoppered tube containing monomer solution, was sonicated for an hour to ensure good swelling/wetting of the PE-PP substrate. A methanol-water (1:1) mixture was used as solvent medium. The system was subjected to a gamma radiation dose of 0.75kGy, at a dose rate of 1.5 kGy/h. Unwanted poly(GMA) homopolymer formed during the mutual irradiation grafting process was removed by washing in a Soxhlet extraction assembly using methanol–water (1:1) mixture as the washing medium. The grafted samples were vacuum dried at 50^0C and stored in a desiccator for further use.

Immobilisation of copper nanoparticles on polymer support

A poly(GMA)-*g*-PE-PP strip of known weight was immersed in an aqueous solution of $CuSO_4.5H_2O$ of pre-determined concentration, to load Cu^{2+} on the polymer support. The solution was stirred for 3 hours to ensure saturated adsorption of Cu^{2+} ions, followed by gentle washing of the strip with ultrapure water to remove physically adsorbed Cu^{2+} ions from the polymer support. Subsequently, the Cu^{2+} ions loaded poly(GMA)-*g*-PE-PP strip was immersed in a 10mM solution of $NaBH_4$ for 30 minutes in ice bath under continuous stirring to ensure complete reduction of Cu^{2+} ions to Cu(0) state**.** Appearance of blackish colouration on the sample surface indicated the formation of Cu nanoparticles.

Characterization

Grafting yield estimation

Radiation grafted poly(GMA)-*g*-PE-PP samples were characterized by Grafting Yield (G.Y.), which was estimated gravimetrically using the relation (1):

G.Y. (%) = [(Weight after grafting - Initial weight)/Initial weight] × 100 (1)

UV Visible Spectrophotometry

A UV-visible spectrophotometer (Evolution 300, Thermoelectron, UK) was used for UV-visible spectral analysis of aqueous samples in the wavelength region of 250-500 nm with resolution of 1.0 nm using quartz cuvette with 10 mm path length.

Fourier Transformed Infrared spectroscopy

Fourier Transformed Infrared (FTIR) spectra of samples were recorded using an IR Affinity-1 spectrometer (Shimadzu, Japan) with diamond single reflectance unit in ATR mode, in wave number region of 400-4000 cm^{-1} with resolution of 4 cm^{-1} and averaged over 50 scans.

Scanning electron microscopy

A SEMART PS-250 (PEMTRON, South Korea) was used for recording SEM micro images at an acceleration voltage of 20.0 kV using secondary electron detector. The sample preparation was carried out by pasting the sample onto the aluminium conducting surface using silver paste and coated with gold using ion sputter coater.

X-Ray fluorescence

XRF analysis of the samples was performed on Field portable X-ray fluorescence (Innov-X Systems Alpha Series ™ FPXRF) system. Sample excitation was carried out using a Tungsten X-ray source (10-40 kV, 10-100 µA). A Si Pin diode detector, having energy resolution of <200 eV, FWHM at 5.95 keV Mn Spectral line, was used for measurement of characteristic X-rays.

Thermogravimetric Analysis (TGA)

In order to study the thermal behaviour of samples, thermogravimetric measurements were performed with TGA/DSC1 system (Mettler Toledo, Switzerland) with gas controller GC100 system (Mettler Toledo, Switzerland). For TG experiments, ~10 mg of the sample was taken in alumina crucible and heated in temperature range of 35–650^{0}C at heating rate of 10^{0}C min^{-1} under inert dynamic high purity nitrogen atmosphere at a flow rate of 50 $ml.min^{-1}$.

Catalytic reduction of PNP: Batch process mode

The catalytic activity of Cu-NiCaR system towards reduction of p-Nitrophenol (PNP) was evaluated by spectrophotometric analysis. Briefly, a reaction mixture comprising of 2.5mL each of 0.03M $NaBH_4$ and 150 µM PNP was brought in contact with a Cu NPs-immobilised-poly(GMA)-g-PE-PP strip of known weight. The reaction was investigated spectrophotometrically by monitoring the decrease in absorbance at 400nm, corresponding to the decrease in PNP concentration. Effect of experimental parameters, such as variation of $CuSO_4.5H_2O$ concentration, PNP concentration, storage stability and repeatability was studied using similar protocol.

Catalytic reduction of PNP: Fixed-bed column mode

The Cu-NICaR system was also tested under continuous flow conditions using a packed fixed bed column reactor in up-flow mode. The experimental setup consisted of a peristaltic pump (Amersham Biosciences-P1), fraction collector (Amersham Biosciences- Frac 920) and a glass column (Pharmacia Fine Chemicals, ID=0.8 cm, h=5.0 cm) packed with 1.0 g of Cu NPs-immobilised-Poly(GMA)-g-PE-PP catalyst, forming a fixed bed with bed volume of ~2.5 cm^3. An aqueous solution containing 1.0 mM PNP and 200mM $NaBH_4$ was passed through the column in up-flow mode at a controlled flow rate of 800 $mL.h^{-1}$. Known volumes of effluent solution were collected from the top of the column in different tubes using automatic fraction collector and, subsequently, analyzed spectrophotometrically for residual PNP concentration.

Results and discussions

Synthesis of poly(GMA)-g-PE-PP Strips

Mutual irradiation grafting process is one of the most versatile and facile techniques for introducing surface functionality onto inert polymers. In this work, epoxy functionalization of the non-woven PE-PP strips was carried out by grafting poly(GMA) via gamma radiation induced mutual irradiation grafting process. These epoxy functionalized poly(GMA)-*g*-PE-PP polymer strips served as the support for Cu^{2+} ions, which were further reduced to subsequently generate Cu nanoparticles.

Effect of absorbed radiation dose on grafting yield

In mutual radiation grafting process, grafting is initiated by free radicals generated upon irradiation of the solvent system comprising of the monomer and the polymer backbone. When the reaction system, comprising a PE-PP strip of known weight immersed in monomer solution of 5% GMA in methanol–water (1:1) mixture, was subjected to different radiation doses, the grafting yield was observed to initially increase linearly up to a radiation dose of 1.3kGy. However, beyond 1.3kGy, the increase in grafting yield was less steep **(Fig. 1)**. This corroborates the results reported earlier by Kumar *et al* [32], wherein the observation was attributed to the exhaustion of monomer molecules at higher doses. Moreover, excess homopolymer formation at high radiation doses, leading to increased viscosity of the grafting medium, also retards the mobility and diffusion of monomer towards the trunk polymer, thereby reducing the grafting yield.

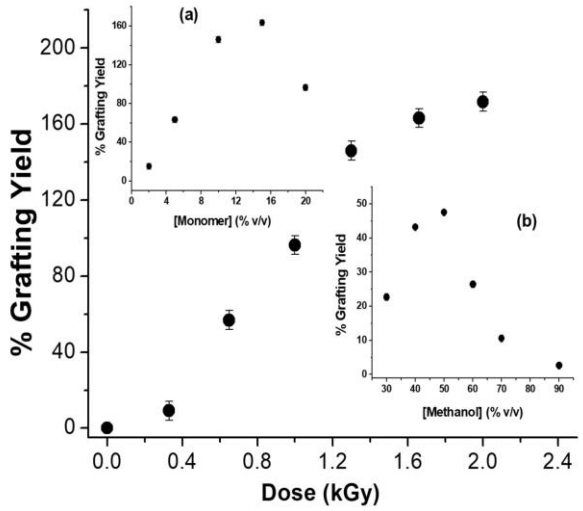

Fig. 1. Variation of grafting yield with absorbed dose (Inset: (a) Variation of Grafting Yield with Monomer Concentration; (b) Variation of grafting yield with solvent composition)

Effect of monomer concentration

Monomer concentration is one of the decisive parameters in determining the radiation grafting yield. **Fig. 1** inset (a) presents the variation of grafting yield with increase in monomer concentration [Dose=0.75kGy, Solvent: methanol–water (1:1), ambience=air] Initially, grafting yield increased with increase in the monomer concentration up to a concentration of 15% (w/v), which is expected since more is the monomer concentration, greater will be the availability of monomers for grafting. The decrease in grafting yield beyond a monomer concentration of 15% can be attributed to the preferential formation of homopolymer at higher monomer concentrations. Additionally, increased monomer concentration also increases the viscosity of the solution, causing further decrease in grafting yield.

Effect of solvent polarity

The effect of solvent polarity on the grafting yield was investigated by carrying out the grafting experiment in solvent media of varying polarity, obtained by varying the methanol:water ratio from 3:7 to 9:1, while keeping other parameters constant ([GMA] = 5%, Dose = 0.75kGy, ambience = air]. It was observed that up to 50% methanol content, grafting yield increased with increase in the methanol content. However, beyond 50%, the yield decreased significantly, as illustrated in **Fig. 1** inset **(b)**. This observation can be explained on the basis of three important parameters i.e. (a) solubility of the monomer and homopolymer in the solvent system (b) swelling/wetting of polymer backbone in the solvent system and (c) quenching of free radicals by the solvent system [33]. Initially, grafting yield increases with increase in methanol content because solubility of GMA and poly(GMA) increases with increase in methanol content; thereby, facilitating approach of monomer towards the polymer backbone. Furthermore, high methanol content results in higher swelling of polymer backbone allowing it to interact with more monomer and increasing grafting yield. However, as the methanol content is increased beyond 50%, quenching of radiolytically generated free radicals (H and OH) by methanol becomes dominant. Since these radicals are the active species in radiation grafting process, decrease in their effective concentration results in drastic decrease in the grafting yield, outweighing the positive effect of the other two parameters. Moreover, when the water concentration in the monomer feed solution becomes very low, the concentration of radiolytically generated reactive radicals (H and OH) in water also goes down, and so does the grafting yield.

Immobilisation of Cu NPs

The synthesis and immobilisation of Cu NPs onto poly(GMA)-*g*-PE-PP strips involves two distinct steps, as illustrated in **Fig. 2**. In the first step, Cu^{2+} precursor ions were loaded onto the polymer support by dipping it in a 10mM $CuSO_4.5H_2O$ aqueous solution. The epoxy groups present on the grafted poly(GMA) chains serve as the anchors for Cu^{2+} ions and prevent the aggregation of the Cu nanoparticles [37,38]. The interaction between $Cu^{2+}$and epoxy functionalized polymer support may arise from the donation of electron from the oxygen atom of epoxy group to the low lying empty orbitals of Cu^{2+} ion. Subsequently, $NaBH_4$, a well known reducing agent, was used to reduce the Cu^{2+} ions to Cu^0 state, a transition marked by the appearance of instant black colouration on the surface of the poly(GMA)-*g*-PE-PP strip [39]. The chemical reaction involved can be represented as:

$$2Cu^{2+} + 4BH_4^- + 12H_2O \rightarrow 2Cu^0 + 14H_2 + 4(BOH)_3 \quad (2)$$

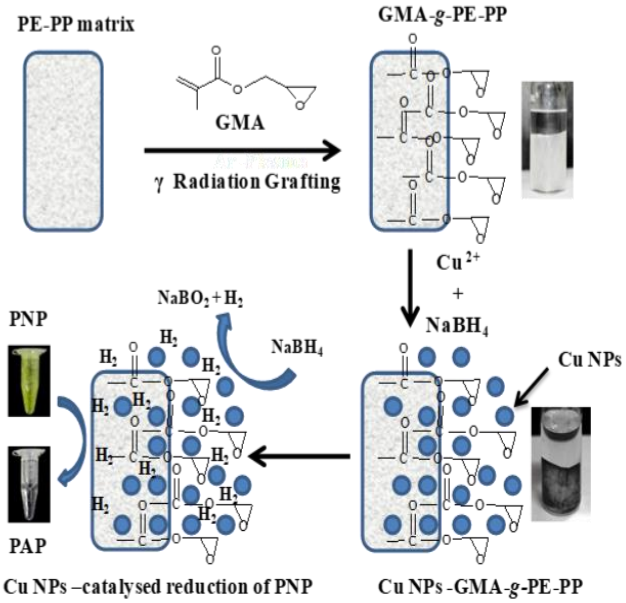

Fig. 2. Schematic of fabrication of Cu-NICaR system.

Characterization of Cu NPs-immobilised-GMA-g-PE-PP strips

Scanning electron microscopy (SEM)

Fig. 3a, 3b and **3c** present the SEM micrographs of pristine PE-PP, poly(GMA)-*g*-PE-PP and Cu NPs-immobilised-poly(GMA)-*g*-PE-PP fibres, respectively. The control PE-PP fibres, as evident from the image, have a smooth morphology **(Fig. 3a)**, which transforms into a rough, uneven surface subsequent to grafting of poly(GMA) chains **(Fig. 3b)**. Moreover, the poly(GMA)-*g*-PE-PP fibres exhibited a significant dimensional increase and change in physical appearance as compared to the control PE-PP fibre, which confirms the grafting of GMA onto PE-PP. SEM image of the Cu NPs-immobilised-poly(GMA)-*g*-PE-PP fibre clearly showed the presence of uniformly distributed spherical nano-particles of Cu **(Fig. 3c)**, which was also confirmed by XRF analysis.

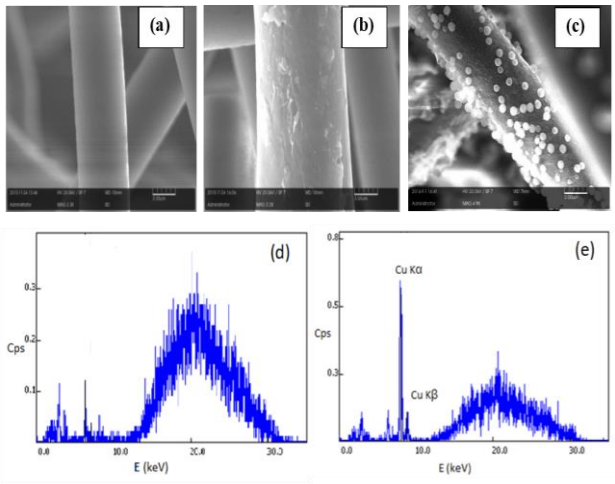

Fig. 3. SEM micrographs of (a) pristine PE-PP fibre and (b) poly(GMA)-*g*-PE-PP (c) Cu NPs-immobilised-poly(GMA)-*g*-PE-PP (d) XRF spectra of poly(GMA)-*g*-PE-PP and (e) XRF spectra of Cu NPs immobilised poly(GMA)-*g*-PE-PP.

XRF analysis

Characteristic X-ray spectra, obtained by XRF analysis, were used to determine the presence of Cu NPs in the sample. **Fig. 3** Inset (d) and **Fig. 3** Inset (e) present the XRF spectra of poly(GMA)-g-PE-PP and Cu NPs immobilised poly(GMA)-g-PE-PP, respectively. The appearance of two distinct additional peaks in Cu NPs immobilised poly(GMA)-*g*-PE-PP at ~ 8.05 keV and ~8.90 keV correspond to Cu K_α and Cu K_β lines, respectively [40]. These clearly indicated the presence of Cu on the sample.

Thermogravimetric Analysis (TGA)

The effect of grafting and subsequent Cu immobilisation on the thermal behaviour of PE-PP polymer backbone was investigated using TGA. Dynamic and derivative thermograms of the samples are shown in **Fig. 4** and Fig. 4 inset, respectively. TGA thermogram of pristine PE-PP exhibited a single sharp decomposition step **(Fig. 4a)** with maximum decomposition temperature at ~ 470^0C (Fig. 4a Inset). Degradation of PE-PP started at ~300ºC and completed at 500^0C [41]. Poly(GMA)-*g*-PE-PP exhibited two stage major decomposition with maximum decomposition temperature at 335^0C (~14% weight loss) and 475^0C (~72 % weight loss) (**Fig. 4b** and Fig. 4b inset), which can be attributed to the sequential degradation of grafted poly(GMA) chains and PE-PP base polymer, respectively. In addition, there was a small weight loss (~5%) at ~225^0C, which can be attributed to the thermal decomposition of pendent gycidyl group. Similarly, a small weight loss step was observed at ~410ºC, attributed to the volatiles generated due to decomposition of grafted chains. These small weight loss steps were observed to be merged with major degradation steps at 335^0C and 475^0C. TGA curve of Cu NPs-immobilised-poly(GMA)-*g*-PE-PP, showed two major decomposition steps similar to the poly(GMA)-g-PE-PP sample (**Fig. 4c** and Fig. 4c inset). The only difference in thermal degradation behaviour of Cu NPs-immobilised-poly(GMA)-g-PE-PP was that the weight loss observed in poly(GMA)-*g*-PE-PP at ~225^0C was not seen. This indicated that the interaction of epoxy group with Cu offered thermal stability to the pendent glycidyl group of the grafted poly(GMA) chains. However, the maximum decomposition temperatures for Cu NPs-immobilised-poly(GMA)-g-PE-PP samples were observed to be lower (~10ºC lower than that for poly(GMA)-*g*-PE-PP) at 325^0C (~20% weight loss) and 465^0C (~72% weight loss). Moreover, the small weight loss step observed for poly(GMA)-*g*-PE-PP sample at 410^0C overlapped with the degradation step at 465^0C. TG analysis indicated that the presence of Cu-NPs in the poly(GMA)-*g*-PE-PP sample improved the thermal degradation behaviour of the closely interacting glycidyl groups, but decreased the thermal stability of grafted chain and the trunk polymer.

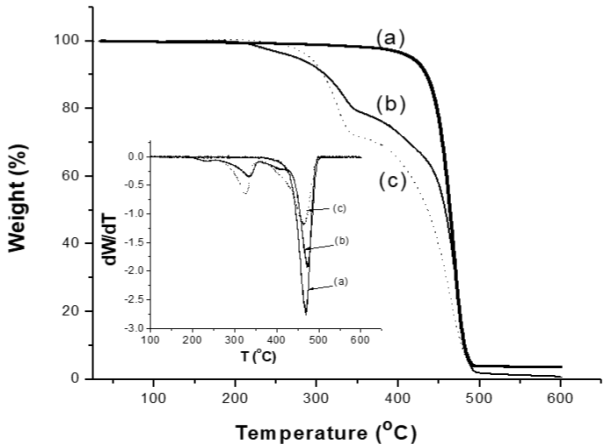

Fig. 4. TGA thermograms of (a) control PE-PP (b) poly(GMA)-*g*-PEPP (c) Cu NPs-immobilised-poly(GMA)-*g*-PE-PP.

Fourier transformed infrared (FTIR) spectroscopy

FTIR analysis was employed to confirm the grafting of poly(GMA) onto PE-PP, as well as to investigate the effect of Cu immobilisation on the poly(GMA)-g-PE-PP samples. As evident from **Fig. 5a**, FTIR spectrum of pristine PE-PP exhibited absorption peaks in the range 2950-2850 cm^{-1}, which correspond to the asymmetric and symmetric stretching modes of CH_2 and CH_3 and another peak in the range of 1500-1450 cm^{-1} corresponding to the scissor deformation modes of CH_2 and CH_3. The FTIR spectrum of poly(GMA)-g-PE-PP sample exhibited additional peaks. The peak at 1725 cm^{-1}, corresponding to carbonyl group and peaks at 905 cm^{-1}, and 1255 cm^{-1}, for the C-O vibrations of epoxy group, as shown in **Fig. 5b**, confirmed the grafting of poly(GMA) onto PE-PP [41,42].

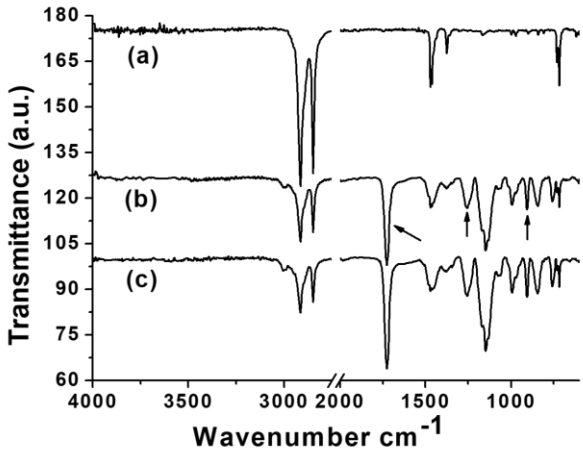

Fig. 5. FTIR spectra of (a) control PE-PP (b) poly(GMA)-*g*-PE-PP (c) Cu NPs-immobilised-poly(GMA)-*g*-PE-PP.

The FTIR spectrum of Cu NPs-immobilised-poly(GMA)-g-PE-PP did not show any appreciable difference as compared to the sample without Cu NPs (fig. 5c). This implied that the interaction between the poly(GMA)-g-PE-PP film and Cu NPs is not strong enough to induce any perceptible shift in the IR peak positions of the groups present in the sample. The changes in thermal behavior can, therefore, solely be ascribed to the packing and confinement of poly(GMA) chains due to interaction with Cu NPs [43]. This mild interaction, however, was optimum to achieve desired extent of immobilisation of Cu NPs and to simultaneously ensure proper functioning of the catalyst support.

Catalytic study

Cu NPs are well known for their catalytic activity towards a range of reduction reactions. The catalytic efficacy of the Cu-NICaR system was determined by spectrophotometrically monitoring the catalytic reduction of p-nitrophenol (PNP) in the presence of $NaBH_4$. An aqueous solution of PNP, initially pale yellow in colour, transforms into a bright yellow coloured solution on addition of $NaBH_4$, due to formation of 4-nitrophenolate ions. The resulting solution shows absorption maxima at 400nm. Reduction of PNP does not take place in presence of $NaBH_4$ alone because of the kinetic barrier between mutually repulsive BH_4^- and phenolate ($C_6H_4NO^-_3$) ions [44]. However, in the presence of catalyst and excess $NaBH_4$, the reduction reaction proceeded rapidly, indicated by the reduction of peak intensity at 400 nm of the UV-vis spectra. **Fig. 6** presents the UV-visible spectra of PNP-$NaBH_4$ reaction system in presence of Cu-NICaR, as a function of reaction time. The reduction of PNP reached completion within 30 minutes of reaction time, as indicated by the complete disappearance/flattening of the peak at 400nm.

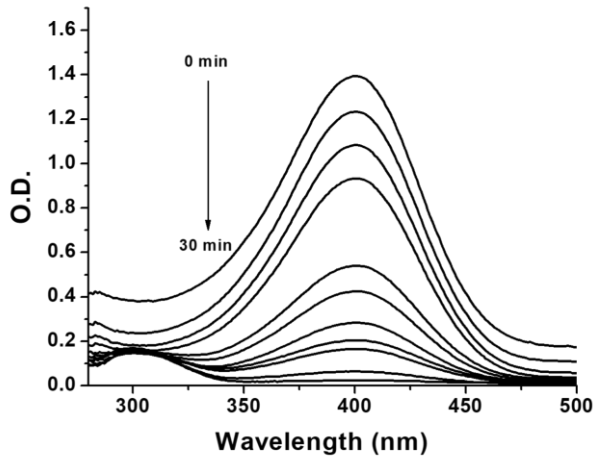

Fig. 6. UV-visible spectra of PNP-$NaBH_4$ reaction system ([PNP] = 75µM, [$NaBH_4$] = 15mM) in presence of Cu-NICaR system, as a function of reaction time.

Kinetic study

The kinetic study of the catalytic reduction of PNP was done by carrying out the reduction reaction with varying concentrations of Cu NPs, loaded on poly(GMA)-*g*-PE-PP. Different initial concentrations of precursor $CuSO_4.5H_2O$ solution were taken to synthesize corresponding Cu NPs loaded poly(GMA)-*g*-PE-PP samples. $NaBH_4$ was added to PNP solution in excess (molar ratio of PNP: $NaBH_4$ =1:200), so as to approximate the reaction kinetics to pseudo first order with respect to PNP. In order to determine the rate constant of the catalytic reduction of PNP, the absorbance values at 400 nm were recorded at different reaction times**.** **Fig. 7** presents the percentage conversion of PNP as a function of reaction time**.** The kinetics of PNP reduction was observed to be quite fast; for example, with 2.5 mM Cu NPs catalyst, ~97 % reduction of 75µM PNP took place within 25 min. The pseudo first order rate constant (k) was estimated using Eqn. 3.

$$ln\ (A_t/A_o) = -k.t \quad (3)$$

where, A_o is the absorbance at t=0, corresponding to initial concentration of PNP (C_0) and A_t is the absorbance at designated time t, corresponding to concentration of PNP (C_t) at time 't'.

Fig. 7 inset (i) presents the pseudo first order kinetic plot, i.e., ln (C_t/ C_o) *Vs* time), for different catalyst concentrations. Good linear fitting (R^2>0.99) of the experimental data to the kinetic model confirmed that the reaction follows pseudo first order reaction kinetics. The pseudo first order rate constants were calculated from the slopes of the plots and are listed in **Table 1**.

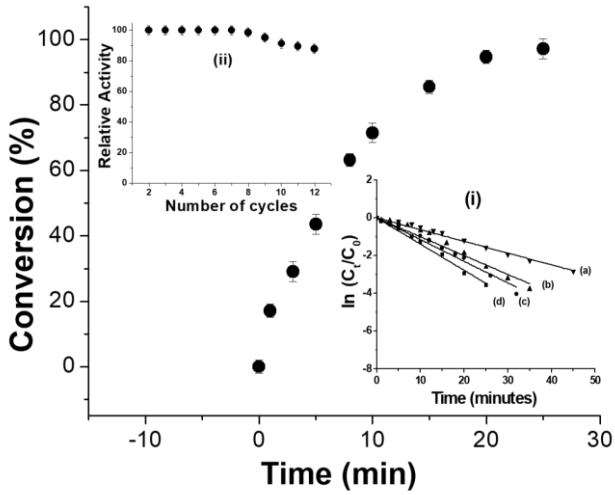

Fig. 7. Reduction of PNP (% conversion) in presence of Cu-NICaR as a function of time. (Inset (i): Plot of ln(C_t/C_0) *vs* time as a function of initial concentration for (a) 0.6mM (b) 0.8mM (c) 1.0mM and (d) 2.5mM [$CuSO_4.5H_2O$]), Inset (ii): Repeatability analysis: relative activity as a function of number of repeated cycles.)

Table 1. Pseudo first order rate constant under varying catalyst concentrations.

S. No.	Initial conc. of Cu^{2+} (mM)	Conc. of PNP (μM)	Pseudo first order rate constant k (s^{-1})
1.	0.6	75	0.0622
2.	0.8	75	0.0996
3.	1.0	75	0.1147
4.	2.5	75	0.1388

The turnover frequency was estimated and compared with some of the recent Cu based catalytic systems reported in literature, as shown in **Table 2** [39, 45, 46].

Table 2. Comparison of catalytic performance of different Cu immobilised catalytic systems for PNP reduction at 298 K.

Catalytic system	Catalyst separation method	TOF/h^{-1}	References
Cu @P(AMPS)	Centrifugation/slow	74.8	N. Sahiner et al (45)
Cu @P(AAGA)	Centrifugation/slow	65.0	S. Butun et al (46)
Cu/CS-CMM	Strip Removal/fast	103.3	S. Haider et al (39)
Cu/P(GMA)-g PEPP	Strip Removal/fast	125.0	Current work

Storage stability and reusability

The primary motive of engineering an immobilised catalytic system is to ensure reusability for multiple cycles with minimum attrition losses and a long shelf life. The Cu-NICaR system was observed to satisfy these criteria. The system could be efficiently reused for more than 12 cycles with less than 4% loss of activity, over a period of 30 days in batch process (**Fig. 7** inset (ii)). Under optimal storage conditions (room temperature, atmospheric pressure) the immobilised catalytic system was found to retain its activity for over 60 days with negligible loss in catalytic activity. This suggested that the catalytic system developed is highly robust and can be economically used for long term practical applications

Catalytic reduction of PNP in packed fixed bed reactor mode

An assessment of the potential industrial applications of Cu-NICaR system for catalytic reduction of PNP was carried out in continuous flow mode using a customized laboratory scale fixed-bed reactor system. The schematic of the setup and experimental data of residual concentration of PNP, relative to the feed concentration (i.e., C/C_o) at different effluent volumes, is presented in **Fig 8**. 1.0 g Cu-NICaR system packed bed reactor, at a flow rate of 800 $mL.h^{-1}$, could completely reduce more than 5000mL of 1.0 mM PNP in aqueous media, without appearance of any breakthrough point. This demonstrated the robustness and efficacy of the Cu-NiCaR system towards potential large scale reduction of PNP to PAP.

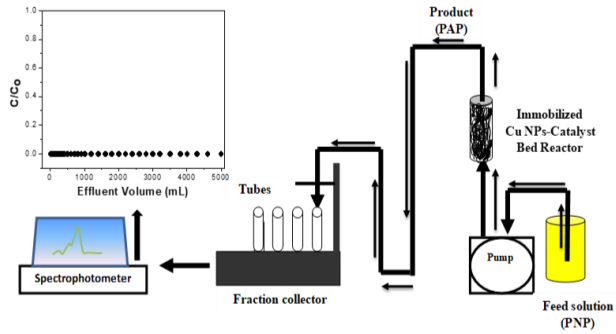

Fig. 8. Schematic of PNP reduction by Cu-NICaR system in fixed bed column flow mode.

Conclusion

A facile radiation technology based methodology has been developed to design functional polymeric templates for immobilisation of Cu NPs. Radiation grafting process was optimised by studying the influence of different reaction parameters on grafting yield. FTIR, TGA, XRF and SEM techniques were employed to characterize the samples and confirm the grafting of epoxy groups and loading of Cu NPs onto radiation grafted poly(GMA)-*g*-PE-PP supports. The

Cu-NICaR system was demonstrated to have high catalytic activity towards p-nitrophenol reduction, besides exhibiting good storage stability and reusability for multiple catalytic cycles without substantial loss in activity. The developed catalytic system has the potential to be employed for multiple cycles in batch reactor mode as well as in continuous flow mode using packed fixed bed column reactor systems, for carrying out large scale catalytic reactions in a commercially viable manner.

References

1. Davis, S. C.; Klabunde, K. J. Chem. Rev. 1982, 82, 153.
2. Misra, N.; Kumar, V.; Rawat, S.; Goel, N. K.; Shelkar, S. A.; Jagannath; Singhal, R. K.; Varshney, L. Environ. Sci. Pollut. Res. 2018. **DOI:** 10.1007/s11356-018-1709-8
3. Nia A. S.; Rana, S.; Döhler, D.; Jirsa, F.; Meister, A.; Guadagno, L.; Koslowski, E.; Bron, M.; Binder, W. H. Chem. - Eur. J. 2015, 21, 10763.
4. Pan, K.; Ming, H.; Yu, H.; Liu, Y.; Kang, Z.; Zhang, H.; Lee, S.-T. Cryst. Res. Technol. 2011, 46, 1167.
5. Allen, S. E.; Walvoord, R. R.; Padilla-Salinas, R.; Kozlowski, M. C. Chem. Rev. 2013, 113, 6234.
6. Kaur, R.; Pal, B. Photocatalysis. Appl. Catal. A 2015, 491, 28.
7. Ben Aissa, M. A.; Tremblay, B.; Andrieux-Ledier, A.; Maisonhaute, E.; Raouafi, N.; Courty, A. Nanoscale 2015, 7, pp 3189−3195.
8. Gonçalves, R. V.; Wojcieszak, R.; Wender, H.; Dias, C. S. B.; Vono, L. L. R.; Eberhardt, D.; Teixeira, S. R.; Rossi, L. M. ACS Appl. Mater. Interfaces 2015, 7, 7987.
9. Zain Mat, N.; Stapley, A. G. F.; Shama, G. Carbohydr. Polym. 2014, 112, 195.
10. Alzahrani, E.; Ahmed, R. A.; Int. J. Electrochem. Sci. 2016, 11, 4712.
11. Zhang, H.; Zhu, Q.; Zhang, Y.; Wang, Y.; Zhao, L.; Yu, B. Adv. Funct. Mater. 2007, 17, 2766.
12. Jeong, S.; Woo, K.; Kim, D.; Lim, S.; Kim, J. S.; Shin, H.; Xia, Y.; Moon, J. *J.* Adv. Funct. Mater. 2008, 18, 679.
13. Surmawar, N. V.; Thakare S. R.; Khaty N. T. Int. J. Green Nanotechnol. 2011, 3, 302.
14. Khanna, P. K.; Kale, T. S.; Koteshwarrao, N.; Satyanarayana, C. V. V. Mater. Chem. Phys. 2008, 110, 21.
15. Ananth, A.; Dharaneedharan, S.; Heo, M.-S.; Mok, Y. S. Chem. Eng. J. 2015, 262, 179.
16. Kawasaki, H.; Kosaka, Y.; Myoujin, Y.; Narushima, T.; Yonezawa, T.; Arakawa, R. Chem. Commun. 2011, 47, 7740.
17. Yu, W.; Xie, H. Q.; Chen, L. F.; Li, Y.; Zhang, C. Nanoscale Res. Lett. 2009, 4, 465.
18. Feng, Z. V.; Lyon, J. L.; Croley, J. S.; Crooks, R. M.; Vanden Bout, D. A.; Stevenson K. J. J. Chem. Educ. 2009, 86, 368.
19. Huang, Z. J.; Li, F. B.; Chen, B. F.; Xue, F.; Chen, G. C.; Yuan, G. G. Appl. Catal. A 2011, 403, 104.
20. Pham, L. Q.; Sohn, J. H.; Kim, C. W.; Park, J. H.; Kang, H. S.; Lee, B. C.; Kang, Y. S. *J.* Colloid Interface Sci. 2012, 365, 103.
21. Kim, Y. H.; Lee, D. K.; Jo, B. G.; Jeong, J. H.; Kang, Y. S. Colloids Surf. A: Physicochem. Eng. Asp. 2006, 284, 364.
22. Joshi, S. S.; Patil, S. F.; Iyer, V.; Mahumuni, S. J. Nanostruct. Mater. 1998, 10, 1135.
23. Park, B. K.; Kim, D.; Jeong, S.; Moon, J.; Kim, J. S. Thin Solid Films, 2007, 515, 7706.
24. Dhas, N. A.; Raj, C. P.; Gedanbken, A. J. Chem Mater. 1998, 10, 1446.
25. Egorova, E.; Revina, A. Colloids Surf. A: Physicochem. Eng. Asp. 2000, 168, 87.
26. Kumar, R. V.; Mastai, Y.; Diamant, Y.; Gedanken, A. J. Mater. Chem. 2001, 11, 1209.
27. Yeh, M. S.; Yang, Y. S.; Lee, Y. P.; Lee, H. F.; Yeh, Y. H.; Yeh, C. S. J. Phys. Chem. B 1999, 103, 6851.
28. Lisiecki, I.; Pileni, M. P. J. Am. Chem. Soc. 1993, 115, 3887.
29. Liu, Z.; Bando, Y. J. Adv. Mater. 2003, 15, 303.
30. Tian, K.; Liu, C.; Yang, H.; Ren, X. Colloids Surf. A: Physicochem. Eng. Asp. 2012, 397, 12.
31. Dang, T. M. D.; Le, T. T. T.; Blanc, E. F.; Dang, M. C. Adv. Nat. Sci. Nanosci. Nanotechnol. 2011, 2, 15009.
32. Kumar, V.; Misra, N.; Goel, N. K., Thakar, R.; Gupta, J.; Varshney, L. RSC Adv. 2016, 6, 2974.
33. Kumar, V.; Bhardwaj, Y. K.; Rawat, K. P.; Sabharwal, S. Radiat. Phys. Chem. 2005, 73, 175.
34. Kumar, V.; Misra, N.; Paul, J.; Dhanawade, B. R.; and Varshney, L. Polymer 2014, 55, 2652.
35. Bhattacharyaa, A.; Misra, B. N. Prog. Polym. Sci. 2004, 29, 767.
36. McLaughlin, W. L.; Boyd, A. K.; Chadwick, K. N.; McDonald, J. C.; Miller, A.; Dosimetry for Radiation Processing; Taylor and Francis, London, 1980.
37. Kou, R.; Shao, Y.; Wang, D.; Engelhard, M. H.; Kwak, J. H.; Wang, J.; Wang, C.; Lin, Y.; Wang, Y.; Aksay, I. A.; Liu, J. Electrochem. Commun., 2009, 11, 954.
38. Kou, R.; Shao, Y.; Mei, D.; Nie, Z.; Wang, D.; Wang, C.; Viswanathan, V. V.; Park, S.; Aksay, I. A.; Lin, Y.; Wang, Y.; Liu, J. J. Am. Chem. Soc. 2011, 133, 2541.
39. Haider, S.; Kamal, T.; Khan, S. B.; Omer, M.; Haider, A.; Khan, F. U.; Asiri, A. M. Appl. Surf. Sci. 2016, 387, 1154.
40. Badawy, S. M.; El-Khashab, R. A.; Nayl, A. A. Bull. Chem. React. Eng. Catal. 2015, 10, 169.
41. Kavaklı, A. P.; Seko, N.; Tamada, M.; Güven, O. J. of App. Polym. Sci. 2007, 105, 1551.
42. Silverstein, R. M.; Bassler, G. C.; Morrill, T. C. (5th Eds.); Spectrometric Identification of Organic Compounds; Wiley Interscience: New York 1991.
43. Gaikwad, P. V.; Sharma, S. K.; Sudarshan, K.; Kumar, V.; Kshirsagar, A.; Pujari, P. K. (2016), Polym. Compos. 2016, **DOI:** 10.1002/pc.24042
44. Saha, S.; Pal, A.; Kundu, S.; Basu, S.; Pal, T. Langmuir 2010, 26, 2885.
45. Sahiner, N.; Ozay, O. Curr. Nanosci. 2012, 8, 367.
46. Butun S.; Sahiner N. Polymer 2011, 52, 4834.

